

## Identification of yrast states in $^{187}\text{Pb}$

A. M. Baxter and A. P. Byrne

*Department of Physics and Theoretical Physics, Faculty of Science, Australian National University, Canberra ACT 0200, Australia*

G. D. Dracoulis, P. M. Davidson, and T. R. McGoram

*Department of Nuclear Physics, RSPHysSE, Australian National University, Canberra ACT 0200, Australia*

P. H. Regan, C. Chandler, W. Gelletly, and C. Wheldon

*Physics Department, University of Surrey, Guildford GU2 5XH, United Kingdom*

R. Julin, J. F. C. Cocks, K. Helariutta, P. Jones, S. Juutinen, H. Kankaanpää, H. Kettunen, P. Kuusiniemi, M. Leino, M. Muikku, and A. Savelius

*Physics Department, University of Jyväskylä, P.O. Box 35, FIN-40351 Jyväskylä, Finland*

R. V. F. Janssens, T. Brown, M. P. Carpenter, C. N. Davids, T. Lauritsen, and D. Nisius

*Physics Division, Argonne National Laboratory, Argonne, Illinois 60439*

P. T. Greenlees

*Oliver Lodge Laboratory, University of Liverpool, Liverpool L69 7ZE, United Kingdom*

(Received 2 July 1998)

$\gamma$ -ray spectroscopy of the high-spin states of the neutron-deficient nucleus  $^{187}\text{Pb}$  has been conducted with the  $^{155}\text{Gd}(^{36}\text{Ar},4n)$  reaction. A cascade of three transitions was deduced from  $\gamma$ - $\gamma$  coincidence data gated by detection of recoiling evaporation residues in a gas-filled recoil separator. In an earlier, separate experiment, two of these  $\gamma$  rays were positively identified with  $^{187}\text{Pb}$  by recoil- $\gamma$  coincidence measurements with a high-resolution, recoil mass spectrometer. From comparison with similar sequences in heavier odd- $A$  lead isotopes, the cascade in  $^{187}\text{Pb}$  is associated with the sequence of three  $E2$  transitions from the yrast  $\frac{25}{2}^+$  level to a low-lying  $\frac{13}{2}^+$  isomer. The variation of excitation energy with mass number of the levels concerned suggests that their structure can be associated with weak coupling of an odd  $i_{13/2}$  neutron to states in the spherical well. However, the possibility that they are influenced by mixing with states in the prolate-deformed well cannot be discounted. [S0556-2813(98)00411-7]

PACS number(s): 21.10.Re, 23.20.Lv, 27.70.+q

### I. INTRODUCTION

Evidence has recently been presented for the observation, at low excitation, of prolate-deformed, rotational bands in the very neutron-deficient, even-mass isotopes  $^{186}\text{Pb}$  [1,2] and  $^{188}\text{Pb}$  [1]. In both cases, the main feature of the level scheme is a single  $\gamma$ -ray cascade with rotationlike spacing for the third and higher excited levels. Its similarity to the well-established, yrast, prolate band observed [3–5] in the corresponding isotones  $^{184}\text{Hg}$  and  $^{186}\text{Hg}$  has been taken as evidence for prolate deformation in lead nuclei. Thus prolate as well as oblate and spherical structures have been observed in the neutron-deficient lead isotopes and, as predicted in several theoretical calculations (e.g., Refs. [6,7]), the prolate band becomes yrast for  $J > 4$  and  $A < 190$ , at least in the even-mass isotopes. In recent studies [8,9] of the  $\alpha$  decay of  $^{192}\text{Po}$ , excited  $0^+$  states in  $^{188}\text{Pb}$  have been reported at excitation energies of 568 [8,9] and 767 keV [9]. These have been identified respectively with the lowest-lying states (albeit mixed) in the oblate- and prolate-deformed wells.

In the very neutron-deficient, odd-mass lead isotopes, very little is known for  $A < 191$ . In  $^{193}\text{Pb}$ , high-spin states have been studied by Lagrange *et al.* [10], Hughes *et al.* [11], and Baldsiefen *et al.* [12]. However, apart from the

superdeformed bands reported by Hughes *et al.* [11], no evidence has been found for significant deformation. Fotiadis *et al.* [13] have very recently presented a level scheme for  $^{191}\text{Pb}$  which likewise shows no indication of deformed structures.

Taking as a guide systematic trends in the odd-mass lead isotopes with  $A \geq 191$ , one would expect the low-lying levels in  $^{187}\text{Pb}$  to correspond to structures in which the odd neutron occupies the single-particle states immediately below the  $N = 126$  shell gap. Characteristic features of the level schemes of these isotopes are a low-spin, odd-parity ground state and the observation, at low excitation ( $\sim 100$  keV), of a very long-lived  $\frac{13}{2}^+$  isomer. Misaelides *et al.* [14] have observed the  $\alpha$  and  $\beta$  decay of two isomers, with similar lifetimes, in  $^{187}\text{Pb}$ . Based on their observed decays, one is associated with the ground state and the other with the expected  $\frac{13}{2}^+$  state. Above the latter isomer, one expects to find, in  $^{187}\text{Pb}$ , a pattern of levels corresponding to weak coupling of the odd  $i_{13/2}$  neutron to the spherical shell-model states in the adjacent even-mass lead isotope. In the heavier odd-mass isotopes, a significant component of this pattern is an isomeric  $\frac{33}{2}^+$  state formed by the coupling of three  $i_{13/2}$  neutrons.

If shape coexistence is present in  $^{187}\text{Pb}$ , competing structures may arise from odd-neutron configurations at either

prolate or oblate deformation. In the isotone  $^{185}\text{Hg}$ , this mechanism gives rise (Hannachi *et al.* [15]) to three strongly coupled rotational bands at prolate deformation and, at oblate deformation, a decoupled band from rotation alignment of the  $i_{13/2}$  neutron. Similar structures are observed in  $^{183}\text{Hg}$  [16] and  $^{187}\text{Hg}$  [17]. In the odd-mass Pb nuclei, the situation is expected to be more complex than in Hg because of the presence of spherical as well as deformed structures.

It is difficult to produce very neutron-deficient nuclei such as  $^{187}\text{Pb}$  by fusion-evaporation reactions owing to the severe competition from fission, and recoil-coincidence techniques are necessary. Thus, in two separate experiments,  $\gamma$ -ray singles and  $\gamma$ - $\gamma$  coincidences were measured, with coincident detection of evaporation residues in one or other of two different recoil mass analyzers, one providing good mass resolution, and the other, high detection efficiency. These provided spectra in which contamination by radiation from fission and Coulomb excitation was greatly reduced, as well as definitive mass identification of the  $\gamma$  rays from evaporation residues.

## II. EXPERIMENTAL METHODS

Excited levels of  $^{187}\text{Pb}$  were populated by bombarding self-supporting  $^{155}\text{Gd}$  targets with beams of  $^{36}\text{Ar}$  ions. In the first experiment, carried out at the Argonne National Laboratory, a beam of 174-MeV  $^{36}\text{Ar}$  ions, from the ATLAS linear accelerator, bombarded a 0.42-mg/cm<sup>2</sup>-thick target enriched to 90.5% in  $^{155}\text{Gd}$ . Evaporation residues recoiling from the target were analyzed and detected in the Argonne fragment mass analyzer (FMA) set at 0° to the beam direction, and  $\gamma$  radiation was detected by ten Compton-suppressed, germanium detectors of the Argonne–Notre Dame BGO  $\gamma$ -ray facility placed around the target.

In a second, similar experiment, a 0.80-mg/cm<sup>2</sup>-thick target, enriched to 92.3% in  $^{155}\text{Gd}$ , was bombarded with a beam of 176-MeV  $^{36}\text{Ar}$  ions from the  $K=130$  cyclotron at the Accelerator Laboratory of the University of Jyväskylä. Evaporation residues recoiling from the target were transported by the gas-filled recoil separator RITU, set at 0° to the beam, to a silicon strip detector at the focal plane.  $\gamma$ -radiation was detected in nineteen Compton-suppressed germanium detectors of the JUROSPHERE array. In the configuration used here this array consisted of fifteen 70%-efficient (EUROGAM Phase I) detectors in the backward hemisphere and four smaller (TESSA) detectors, two at 79°, and two at 101° to the beam direction. The two experiments were distinguished mainly by the characteristics of the two magnetic analyzers: the FMA has mass resolution sufficient to provide definitive mass identification of the evaporation residues, whereas RITU, although having much poorer mass resolution, is about an order of magnitude more efficient at transporting the residues.

The FMA (Davids *et al.* [18]) is a recoil mass spectrometer which produces dispersion in the ratio mass/charge of the reaction products. Recoiling ions which reached the focal plane were detected by a multiwire proportional counter (MWPC) which produced  $\Delta E$  and focal-plane-position signals. Other details of the experimental arrangement using the FMA may be found in Ref. [2].

The recoil separator RITU (Leino *et al.* [19]) transports

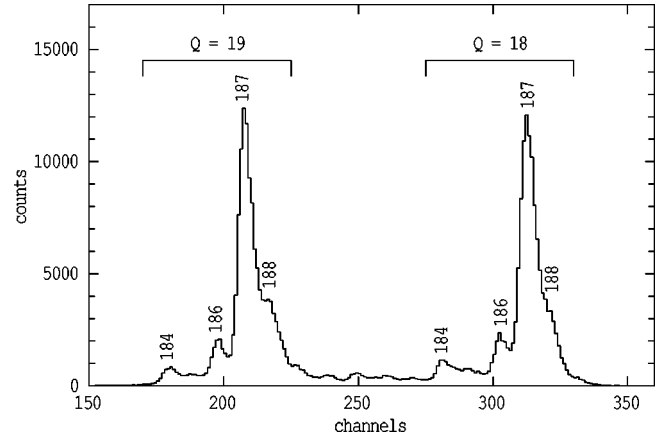


FIG. 1. Mass spectrum from projection onto the  $X_{\text{MWPC}}$  axis of the matrix of  $X_{\text{MWPC}}$  of the FMA vs  $E_\gamma$ . Peaks are labeled by the mass number of the recoiling ions and fall into two groups corresponding to charge states  $Q=18$  and  $19$ .

reaction products from the target to a silicon strip detector at its focal plane with an efficiency as high as 50%. Although this high efficiency is obtained at the expense of mass resolving power, the device was still capable, in the present experiment, of separating evaporation residues from beam particles and fission fragments. The silicon strip detector provided signals giving the energy, position and detection time of particles arriving at the focal plane. The energies of  $\gamma$  rays in coincidence with particles detected at the focal plane of RITU (after allowing for their transit time) were also recorded. Both recoil-gated  $\gamma$  singles and  $\gamma$ - $\gamma$  coincidence data were acquired. When using a silicon strip detector at the focal plane, there exists the capability of uniquely identifying evaporation residues by observation of their time-correlated  $\alpha$  decays. However the half-life (18.3 s, Ref. [14]) of the putative  $\frac{13}{2}^+$  isomer in  $^{187}\text{Pb}$  is too long for this technique to be feasible in the present case. In addition  $\beta$  decay has been observed [14] to compete significantly with the  $\alpha$  branch in the decay of this level.

## III. DATA ANALYSIS AND RESULTS

### A. Recoil- $\gamma$ data with the FMA

The mass spectrum of recoil ions detected at the focal plane of the FMA is shown in Fig. 1. The electric and magnetic fields of the FMA were set so that the central trajectory corresponded to mass-187 ions, and both  $18^+$  and  $19^+$  charge states of the evaporation residues fitted within the acceptance aperture of the MWPC. The spectrum in Fig. 1 is a total projection onto the position axis of a matrix of  $X_{\text{MWPC}}$  vs  $E_\gamma$ , corrected for Doppler shifts. In constructing this matrix, it was required that the transit time of the ions through the FMA (1.5  $\mu\text{s}$ ) and the  $\Delta E$  pulse from the MWPC both correspond to evaporation residues. The mass resolving power  $M/\Delta M$  in the spectrum (Fig. 1) is approximately 250 and is sufficient that peaks corresponding to adjacent mass values can be clearly discerned even though they are not completely resolved. There is a tail on the high-mass side of the peaks arising from second-order aberrations in the FMA, which, in order to achieve the greatest yield, was used with maximum aperture.

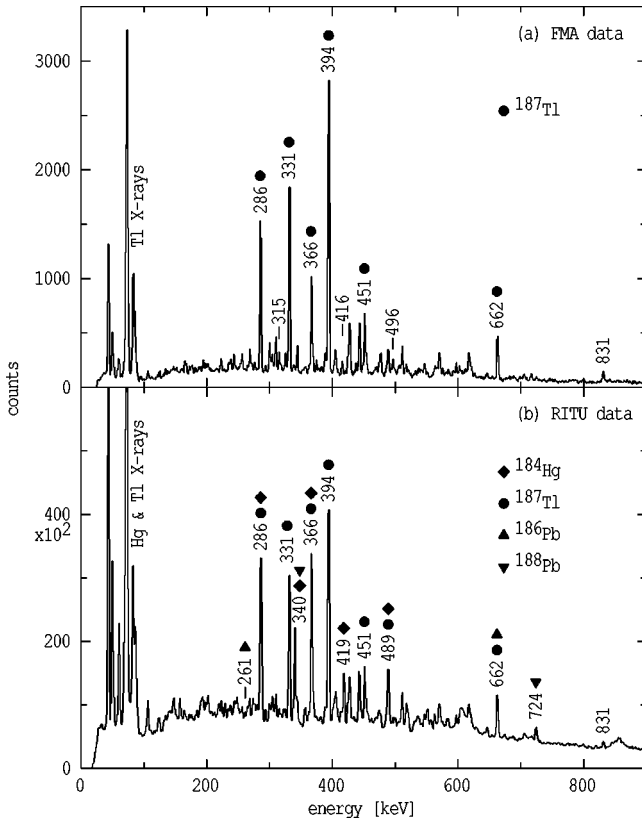


FIG. 2. (a) Part of the  $\gamma$ -ray spectrum gated by the two mass-187 peaks in the  $X_{\text{MWPC}}$  spectrum of the  $^{155}\text{Gd}+^{36}\text{Ar}$  reaction. Almost all the lines of significant intensity (apart from x rays) can be identified with known transitions in  $^{187}\text{Tl}$  and the more prominent ones are labeled. As discussed in the text, all those that cannot be identified with  $^{187}\text{Tl}$  are regarded as candidates for transitions in  $^{187}\text{Pb}$  and the strongest of them are labeled by their energies only. (b) Total projection of the matrix of  $\gamma$ - $\gamma$  coincidences gated by detection of evaporation residues at the focal plane of the recoil separator RITU. The more prominent peaks are labeled by their energies and the nucleus to which they are assigned; the 831 keV line is discussed in the text.

The spectrum in Fig. 2(a) is a projection on the  $E_\gamma$  axis of the  $X_{\text{MWPC}}$  vs  $E_\gamma$  matrix with gates on the two mass-187 peaks in the mass spectrum shown in Fig. 1. This spectrum is dominated by transitions in  $^{187}\text{Tl}$  [20] and peaks corresponding to x rays from thallium and gadolinium. (The Gd x rays presumably arise from chance coincidences or coincidences with beam particles scattered through the FMA.) There is no significant contamination of this spectrum with  $\gamma$  rays from nuclei with  $A \neq 187$ . Furthermore, no  $\gamma$ -ray lines corresponding to known transitions in any nucleus having  $A = 187$  and  $Z < 81$ , are observed, so it is concluded that the remaining lines are candidates for transitions in  $^{187}\text{Pb}$ . The strongest of them have energies of 315.0, 416.0, 424.0, 495.5 and 830.5 keV and four of them are labeled in Fig. 2(a). All these five lines are stronger than the weakest  $^{187}\text{Tl}$   $\gamma$  rays identified in this spectrum so it is very unlikely that any of them belong in the decay scheme [20] of that nucleus. However, they were not sufficiently strong for it to be possible to determine their coincidence relationships from mass-gated,  $\gamma$ - $\gamma$  coincidence data.

In Fig. 3 the four spectra show the identification of certain

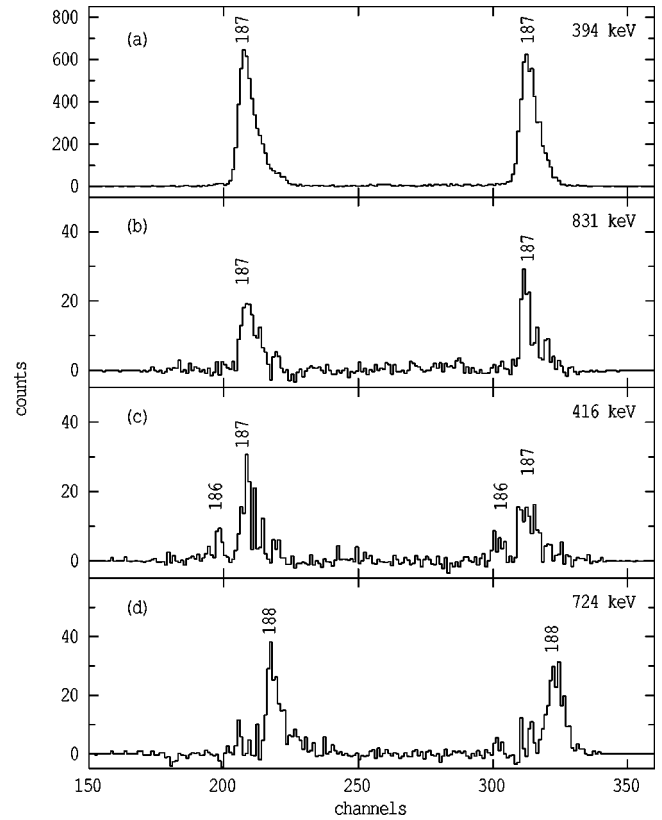


FIG. 3. Mass spectra from projections onto the  $X_{\text{MWPC}}$  axis of the matrix of  $X_{\text{MWPC}}$  vs  $E_\gamma$  with gates on certain  $\gamma$ -ray lines as discussed in the text. Peaks are labeled by the mass number to which they correspond.

$\gamma$ -ray lines with evaporation residues of a particular mass number, produced by projection onto the mass axis from the  $X_{\text{MWPC}}$  vs  $E_\gamma$  matrix. In Fig. 3(a) the gate is on the strong 394 keV line [see Fig. 2(a)] arising from the 392.8 and 394.1 keV transitions in  $^{187}\text{Tl}$  [20]. This spectrum gives the line shape in the mass spectrum for recoil ions of a single mass ( $A = 187$ ) and provides a reference for the other mass spectra. The mass spectra corresponding to two of the candidates for  $\gamma$ -ray transitions in  $^{187}\text{Pb}$  are shown in Figs. 3(b) and 3(c); these show clearly that most of the intensity of these two lines is associated with  $A = 187$  recoils. In the case of the 416 keV gate, there are also suggestions of weak peaks corresponding to  $A = 186$ ; presumably these correspond to the 415 keV transition in  $^{186}\text{Pb}$  [2]. Finally, to illustrate the mass discrimination, the mass spectrum corresponding to the 724 keV,  $2^+$  to  $0^+$  transition in  $^{188}\text{Pb}$  [1] is shown in Fig. 3(d).

## B. Recoil- $\gamma$ - $\gamma$ data with RITU and $\alpha$ decay of evaporation residues

### 1. $\alpha$ -decay data

Figure 4 shows a spectrum of  $\alpha$  particles detected in the silicon strip detector of the recoil separator RITU during a short segment of the run. The most intense and highest-energy group in this spectrum is attributed to the decay from the ground state of  $^{186}\text{Pb}$ , previously reported by Le Beyec *et al.* [21] and Toth *et al.* [22]. The  $\alpha$ -decay branching ratios given by these two groups are in conflict: 2.4% in the former work and 100% in the latter. The value of Toth *et al.* (100%)

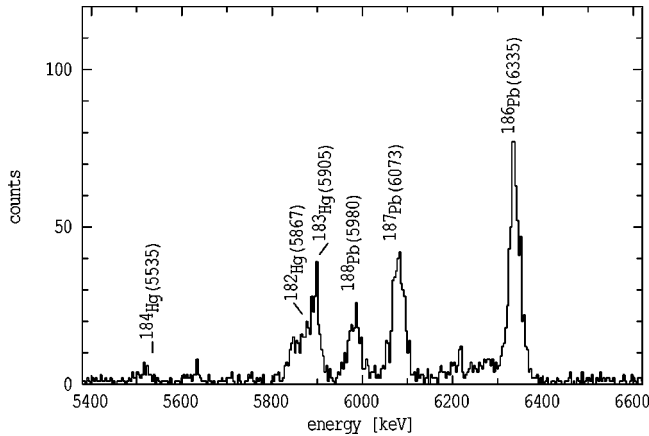


FIG. 4. Part of the spectrum of  $\alpha$  particles from the decay of evaporation residues at the focal plane of the recoil separator RITU. Peaks are labeled by the parent nucleus and the corresponding  $\alpha$ -particle energy in keV. The energy scale was calibrated by a linear fit to the  $^{186}\text{Pb}$ (6335),  $^{187}\text{Pb}$ (6073), and  $^{188}\text{Pb}$ (5980) peaks and the expected positions of the other peaks were predicted with this calibration.

appears to be the more reliable. The peak at 5980 keV in Fig. 4, identified with the decay of  $^{188}\text{Pb}$  (see, for example, Ref. [22]) is about one-third of the size of the  $^{186}\text{Pb}$  peak, notwithstanding the fact that  $^{186}\text{Pb}$   $\gamma$  rays were found to be slightly less intense in the recoil-gated  $\gamma$ - $\gamma$  data than those of  $^{188}\text{Pb}$ . This can be attributed to the  $\alpha$ -decay branching ratios of 22% and 100% for  $^{188}\text{Pb}$  and  $^{186}\text{Pb}$  [22], respectively. Note, however, that the comparison of  $\gamma$ -decay intensities in the two nuclei takes no account of the unobserved fractions of the decay strengths which may depopulate long-lived isomers.

The second strongest peak in the spectrum in Fig. 4, at 6073 keV, is identified with the  $\alpha$  decay of the putative  $J^\pi = \frac{13}{2}^+$  isomer in  $^{187}\text{Pb}$ , previously reported by Misaelides *et al.* [14] and Le Beyec *et al.* [21]. At first sight its prominence is surprising in view of the small  $\alpha$ -decay branching ratio of 2.0% deduced by Le Beyec *et al.* and the fact that, in the present work, the intensities of the proposed  $^{187}\text{Pb}$   $\gamma$  rays were found to be only about one-third of those of comparable  $^{186}\text{Pb}$  or  $^{188}\text{Pb}$  lines. However, as discussed above, doubt has been cast on the validity of the small  $\alpha$ -decay branching ratio given by Le Beyec *et al.* in the case of  $^{186}\text{Pb}$  so it seems possible that the  $^{187}\text{Pb}$   $\alpha$ -decay branching ratio may be much greater than the 2.0% reported by these workers. Even though Misaelides *et al.* [14] observed both  $\alpha$ - and  $\beta$ -decay branches from the  $(\frac{13}{2}^+)$  isomer in  $^{187}\text{Pb}$ , branching ratios were not given in that work. Even if the  $\alpha$ -decay branch is as large as, say, 50%, the strength of the  $^{187}\text{Pb}$   $\alpha$ -particle group in Fig. 4, relative to those of  $^{186}\text{Pb}$  and  $^{188}\text{Pb}$  is larger than would be expected from a comparison of the intensities of their  $\gamma$  rays in the recoil-gated  $\gamma$ - $\gamma$  data discussed below. This strongly suggests that a substantial fraction of the  $^{187}\text{Pb}$   $\gamma$ -decay strength may pass through another isomer, lying at higher excitation than the one whose  $\alpha$  decay is observed, and whose lifetime is long enough ( $> \sim 20$  ns) that most of the decays take place after the nuclei have recoiled out of the field of view of the Ge detectors.

The expected positions of other  $\alpha$ -particle groups which could have detectable intensity are shown in Fig. 4. The predictions are based on an internal energy calibration using the three prominent peaks identified in the foregoing discussion with  $^{186,187,188}\text{Pb}$ , and  $\alpha$ -decay energies of  $5535 \pm 15$  keV [23] for  $^{184}\text{Hg}$ , and  $5867 \pm 5$  keV and  $5905 \pm 5$  keV, respectively, [24] for  $^{182}\text{Hg}$  and  $^{183}\text{Hg}$ . Although the most prominent nuclide in the  $\gamma$ -ray data is  $^{187}\text{Tl}$ , the  $5528 \pm 10$  keV  $\alpha$ -decay branch [25] from the  $9/2^-$  isomer in this nucleus is expected to be very weak or undetectable in the present experiment owing to the small (0.15% [26])  $\alpha$ -decay branching ratio.

## 2. The recoil $\gamma$ - $\gamma$ data

The recoil  $\gamma$ - $\gamma$  data were sorted to produce an  $E_\gamma$  vs  $E_\gamma$  matrix of coincidences within a 200 ns window, gated by the requirement of the detection of the corresponding evaporation residue at the focal plane of RITU. (The transit time of the residues through RITU was approximately  $0.9 \mu\text{s}$ .) The spectrum in Fig. 2(b) is a total projection of this recoil-gated  $\gamma$ - $\gamma$  matrix. The strongest lines can be attributed to transitions in  $^{187}\text{Tl}$  [20] and  $^{184}\text{Hg}$  [3], and to x rays from thallium, mercury, and gadolinium. Lines corresponding to transitions in  $^{186}\text{Pb}$  [1,2] and  $^{188}\text{Pb}$  [1] are also present. Since essentially all evaporation residues contribute to this spectrum, it is more complex than that obtained with the FMA [see Fig. 2(a)] despite the requirement of  $\gamma$ - $\gamma$  coincidences in the former case. In particular, the peak-to-continuum ratio in Fig. 2(b) is worse and consequently, of the  $^{187}\text{Pb}$  candidates, only the 831 keV line could readily be discerned.

A projection from the recoil-gated  $\gamma$ - $\gamma$  matrix, with a gate on the 831 keV line [Fig. 5(a)], shows coincidences with lines at 318, 416, and 476 keV and with Pb x rays. (The peaks at energies less than 70 keV correspond to gadolinium and tungsten x rays, the latter from fluorescence in detector shielding.) Figure 5(b) shows the projection with a gate on the 416 keV line, after subtraction of contamination from lines in coincidence with the 419 keV transition in  $^{184}\text{Hg}$  [3]. The 416 keV  $\gamma$  rays are in coincidence with lines at 476 and 831 keV; the remaining lines can be identified with  $^{186}\text{Pb}$   $\gamma$  rays [1,2], in coincidence with the 415 keV transition in that nucleus. It was not possible to remove these contaminants owing to the low statistical accuracy and the proximity of other overlapping peaks. The gate on the 476 keV line [Fig. 5(c)] confirms the mutual coincidence relationship between the 831, 416, and 476 keV  $\gamma$ -ray lines. The  $^{187}\text{Tl}$  lines in the 476 keV gate arise from contamination in the gate from the 476.9 and 477.3 keV lines in that nucleus [20]. The 318 keV gate shows a very weak line near 830 keV and thallium x rays but otherwise is essentially featureless.

We thus deduce from the recoil-gated  $\gamma$ - $\gamma$  coincidence data that the 831, 416, and 476 keV lines form a cascade. One of them (the 831 keV line) is in coincidence with lead x rays, and the mass-gated data obtained with the FMA demonstrate that the 831 and 416 keV lines are associated with  $A = 187$  recoils. The cascade is therefore unambiguously assigned to  $^{187}\text{Pb}$  and is shown as an inset in Fig. 5(a) with the ordering of the transitions determined by relative intensities. On the basis of systematic trends, it is assumed that the lowest level shown in the cascade is the low-lying  $\frac{13}{2}^+$  isomer observed (e.g., Ref. [10]) in the heavier, odd-mass, lead iso-

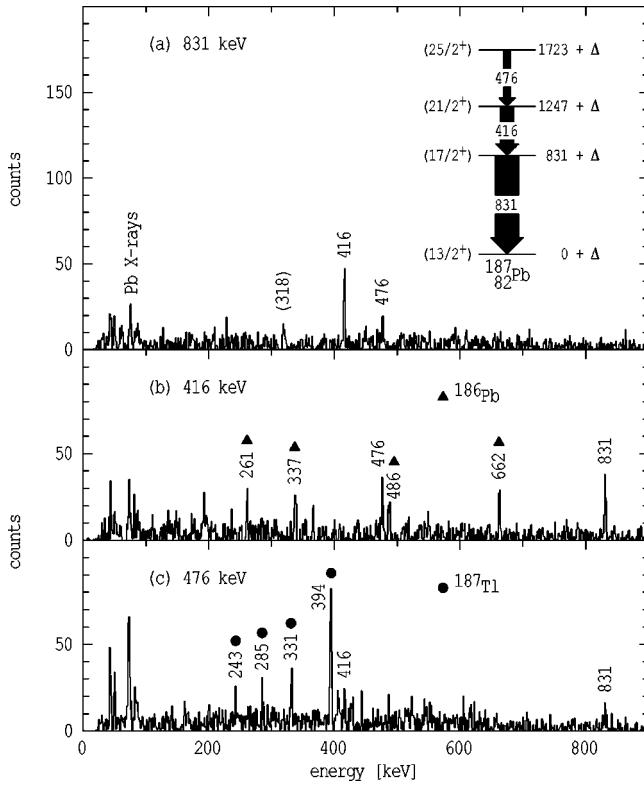


FIG. 5. Projections from the recoil-gated  $\gamma$ - $\gamma$  matrix with gates on the 831, 416, and 476 keV  $\gamma$ -ray lines which, as discussed in the text, are identified with transitions in  $^{187}\text{Pb}$ . Contaminant lines from other nuclides are labeled by their energies and the nucleus responsible. The partial level scheme for  $^{187}\text{Pb}$  deduced in the present work is shown as an inset in the top panel. The widths of the arrows indicate the relative intensities of the corresponding  $\gamma$  rays.

topes and, also from these trends, its excitation energy (denoted by  $\Delta$  in Fig. 5) is expected to be about 100 keV.

The angular distributions of the  $^{187}\text{Pb}$   $\gamma$  rays in the recoil- $\gamma$  data were isotropic within statistical uncertainties so it was not possible to obtain any information on spins from these data. The spins and parities tentatively assigned to higher levels in the inset to Fig. 5(a) are, similar to those of the lowest level, based on comparisons with the heavier odd-mass lead isotopes and are discussed further in the following section.

#### IV. DISCUSSION

Figure 6 shows plots against mass number  $A$ , from  $A = 186$  to 200, of the excitation energies of the yrast  $2^+$ ,  $4^+$ , and  $6^+$  levels in the even- $A$  isotopes of lead and of the excitation energies, relative to the  $\frac{13}{2}^+$  isomer, of the yrast  $\frac{17}{2}^+$ ,  $\frac{21}{2}^+$ , and  $\frac{25}{2}^+$  levels in the odd- $A$  isotopes. With the exception of the  $6^+$  levels in  $^{196,198,200}\text{Pb}$ , which have not yet been identified, the spin and parity assignments are well established for all these levels in the isotopes with  $A \geq 192$ . For  $A \leq 191$ , the assignments are less certain and, particularly in the very light isotopes, are based largely on extrapolation of systematic trends in the heavier isotopes.

It can be seen in Fig. 6 that, for  $A \geq 191$ , the energies of the  $\frac{17}{2}^+$  levels in the odd- $A$  isotopes follow closely those of the  $2^+$  levels in the even- $A$  isotopes. Likewise, there is a

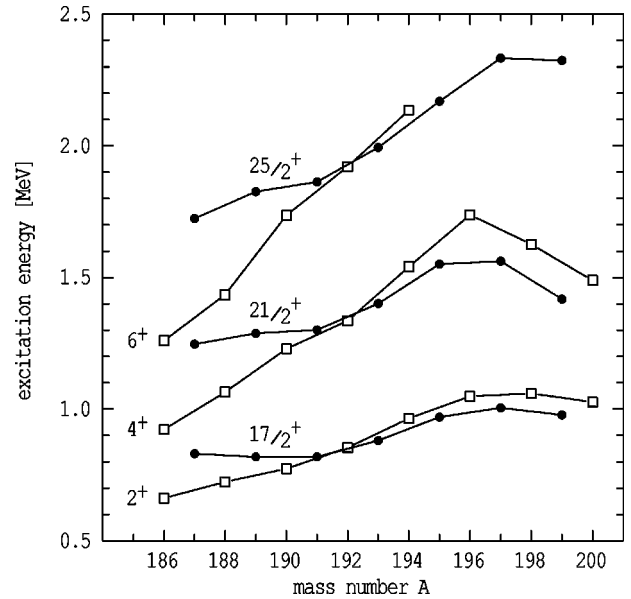


FIG. 6. Plots against mass number  $A$  of the excitation energies of the yrast  $2^+$ ,  $4^+$ , and  $6^+$  states in the even-mass lead isotopes with  $A = 186$  to 200, and of the excitation energies relative to the  $\frac{13}{2}^+$  isomer of the yrast  $\frac{17}{2}^+$ ,  $\frac{21}{2}^+$ , and  $\frac{25}{2}^+$  states in the odd-mass lead isotopes with  $A = 187$  to 199. The main sources of the data plotted are  $^{186}\text{Pb}$  [1,2],  $^{187}\text{Pb}$ , present work,  $^{188}\text{Pb}$  [1],  $^{189}\text{Pb}$  [27],  $^{190}\text{Pb}$  [28],  $^{191}\text{Pb}$  [13],  $^{192}\text{Pb}$  [10],  $^{193}\text{Pb}$  [10,12],  $^{194}\text{Pb}$  [29,30],  $^{195}\text{Pb}$  [29,31],  $^{196}\text{Pb}$  [32],  $^{197,198}\text{Pb}$  [33],  $^{199}\text{Pb}$  [34,35], and  $^{200}\text{Pb}$  [35].

similar dependence on  $A$ , for  $A \geq 191$ , of the energies of the  $\frac{21}{2}^+$  and  $4^+$  levels and of the  $\frac{25}{2}^+$  and  $6^+$  levels. This is the behavior one would expect if the levels in the odd- $A$  cases arise from the weak coupling of an  $i_{13/2}$  neutron (or neutron hole) to the  $2^+$ ,  $4^+$ , and  $6^+$  states in the spherical well of the neighboring even- $A$  core. The similarity is closest in  $^{191}\text{Pb}$  and  $^{193}\text{Pb}$ .

For  $A < 191$ , however, there is a sharp divergence between the trends in the odd- and even- $A$  cases. The energies of the  $2^+$ ,  $4^+$ , and  $6^+$  levels continue to decrease with decreasing  $A$  reflecting the predicted [6,7] influence of the prolate well near midshell. On the other hand, the energies of the  $\frac{17}{2}^+$ ,  $\frac{21}{2}^+$ , and  $\frac{25}{2}^+$  levels remain essentially constant with  $A$  for  $A < 191$ . This behavior is consistent with these levels arising, as for  $A \geq 191$ , from weak coupling of the odd neutron to the spherical states in the even-mass isotopes. The latter states have not been observed in  $^{186}\text{Pb}$  and  $^{188}\text{Pb}$  presumably because they are not yrast. If, in  $^{187}\text{Pb}$ , a  $\frac{9}{2}^+$  [624] prolate band, for example, were to compete with the spherical states, and this band had significant signature splitting as it does in the isotope  $^{185}\text{Hg}$  [15], then it is possible that only a single sequence of transitions would be observed and this would not distinguish between the spherical and deformed structures. The clearest evidence for prolate deformation may be in the observation of transitions in both signatures of the  $\frac{9}{2}^+$  [624] band or in the other prolate bands. Now that the present work has positively identified transitions between the lower yrast levels in  $^{187}\text{Pb}$  future studies can be focussed on extending the level scheme along these lines. Measurements on the decay of the expected isomeric spherical states should

also shed light on the degree to which shape coexistence influences the yrast structure of  $^{187}\text{Pb}$ .

### ACKNOWLEDGMENTS

This work was supported in part by the Australian Government's Department of Industry, Science and Technology

and the Australian Research Council, by the U.S. Department of Energy, Nuclear Physics Division, under Contract No. W-31-109-ENG-38, by the Access to Large Scale Facilities Program under the Training and Mobility of Researchers Program of the European Union, and by the Academy of Finland. P.J. acknowledges the receipt of a Marie Curie Research Training Grant and C.C. and C.W. acknowledge receipt of UK EPSRC studentships.

- 
- [1] J. Heese, K. H. Maier, H. Grawe, J. Grebosz, H. Kluge, W. Meczynski, M. Schramm, R. Schubart, K. Spohr, and J. Styczen, *Phys. Lett. B* **302**, 390 (1993).
- [2] A. M. Baxter, A. P. Byrne, G. D. Dracoulis, R. V. F. Janssens, I. G. Bearden, R. G. Henry, D. Nisius, C. N. Davids, T. L. Khoo, T. Lauritsen, H. Pentillä, D. J. Henderson, and M. P. Carpenter, *Phys. Rev. C* **48**, R2140 (1993).
- [3] J. K. Deng, W. C. Ma, J. H. Hamilton, A. V. Ramayya, J. Kormicki, W. B. Gao, X. Zhao, D. T. Shi, I. Y. Lee, J. D. Garrett, N. R. Johnson, D. Winchell, M. Halbert, and C. Baktash, *Phys. Rev. C* **52**, 595 (1995).
- [4] W. C. Ma, J. H. Hamilton, A. V. Ramayya, L. Chaturvedi, J. K. Deng, W. B. Gao, Y. R. Chang, J. Kormicki, X. W. Zhao, N. R. Johnson, J. D. Garrett, I. Y. Lee, C. Baktash, F. K. McGowan, W. Nazarewicz, and R. Wyss, *Phys. Rev. C* **47**, R5 (1993).
- [5] M. G. Porquet, G. Bastin, C. Bourgeois, A. Korichi, N. Perrin, H. Sergolle, and F. A. Beck, *J. Phys. G* **18**, L29 (1992).
- [6] F. R. May, V. V. Pashkevich, and S. Frauendorf, *Phys. Lett.* **68B**, 113 (1977).
- [7] R. Bengtsson and W. Nazarewicz, *Z. Phys. A* **334**, 269 (1989).
- [8] N. Bijmens *et al.*, *Z. Phys. A* **356**, 3 (1996).
- [9] R. G. Allat *et al.*, *Phys. Lett. B* (to be published).
- [10] J. M. Lagrange, M. Pautrat, J. S. Dionisio, Ch. Vieu, and J. Vanhorenbeeck, *Nucl. Phys. A* **530**, 437 (1991).
- [11] J. R. Hughes *et al.*, *Phys. Rev. C* **51**, R447 (1995).
- [12] G. Baldsiefen *et al.*, *Phys. Rev. C* **54**, 1106 (1996).
- [13] N. Fotiades *et al.*, *Phys. Rev. C* **57**, 1624 (1998).
- [14] P. Misaelides, P. Tidemand-Petersson, U. J. Schrewe, I. S. Grant, R. Kirchner, O. Klepper, I. C. Malcolm, P. J. Nolan, E. Roeckl, W.-D. Schmidt-Ott, and J. L. Wood, *Z. Phys. A* **301**, 199 (1981).
- [15] F. Hannachi, G. Bastin, M. G. Porquet, J. B. Thibaud, C. Bourgeois, L. Hildingsson, N. Perrin, H. Sergolle, F. A. Beck, and J. C. Merdinger, *Z. Phys. A* **330**, 15 (1988).
- [16] G. J. Lane, G. D. Dracoulis, A. P. Byrne, S. S. Anderssen, P. M. Davidson, B. Fabricius, T. Kibédi, A. E. Stuchbery, and A. M. Baxter, *Nucl. Phys. A* **589**, 129 (1995).
- [17] F. Hannachi, G. Bastin, M. G. Porquet, C. Schüick, J. B. Thibaud, C. Bourgeois, L. Hildingsson, D. Jerrestam, N. Perrin, H. Sergolle, F. A. Beck, T. Byrski, J. C. Merdinger, and J. Dudek, *Nucl. Phys. A* **481**, 135 (1988).
- [18] C. N. Davids and J. D. Larson, *Nucl. Instrum. Methods Phys. Res. B* **40/41**, 1224 (1989); C. N. Davids, B. B. Back, K. Bindra, D. J. Henderson, W. Kutschera, T. Lauritsen, Y. Nagame, P. Sugathan, A. V. Ramayya, and W. B. Walters, *ibid.* **70**, 358 (1992).
- [19] M. Leino, J. Äystö, T. Enqvist, P. Heikkinen, A. Jokinen, M. Nurmi, A. Ostrowski, W. H. Trzaska, J. Uusitalo, K. Eskola, P. Armbruster, and V. Ninov, *Nucl. Instrum. Methods Phys. Res. B* **99**, 653 (1995).
- [20] G. J. Lane, G. D. Dracoulis, A. P. Byrne, P. M. Walker, A. M. Baxter, J. A. Sheikh, and W. Nazarewicz, *Nucl. Phys. A* **586**, 316 (1995).
- [21] Y. Le Beyec, M. Lefort, J. Livet, N. T. Porile, and A. Siivola, *Phys. Rev. C* **9**, 1091 (1974).
- [22] K. Toth, Y. A. Ellis-Akovi, C. R. Bingham, D. M. Moltz, D. C. Sousa, H. K. Carter, R. L. Mlekodaj, and E. H. Spejewski, *Phys. Rev. Lett.* **53**, 1623 (1984).
- [23] P. G. Hansen, H. L. Nielsen, K. Wilsky, M. Alpsten, M. Finger, A. Lindahl, R. A. Naumann, and O. B. Nielsen, *Nucl. Phys. A* **148**, 249 (1970).
- [24] E. Hagberg, P. G. Hansen, P. Hornshøj, B. Jonson, S. Mattsson, and P. Tidemand-Petersson, *Nucl. Phys. A* **318**, 29 (1979).
- [25] U. J. Schrewe, P. Tidemand-Petersson, G. M. Gowdy, R. Kirchner, O. Klepper, A. Plochocki, W. Reisdorf, E. Roeckl, J. L. Wood, J. Zylicz, R. Fass, and D. Schardt, *Phys. Lett.* **91B**, 46 (1980).
- [26] J. Wauters, P. Decroock, P. Dendooven, M. Huyse, G. Reusen, and P. Van Duppen, *Z. Phys. A* **339**, 533 (1991).
- [27] A. M. Baxter *et al.*, Department of Nuclear Physics, Australian National University, annual report, 1996 (unpublished), p. 30.
- [28] A. M. Baxter, A. P. Byrne, G. D. Dracoulis, S. Bayer, and N. S. Bowden, Department of Nuclear Physics, Australian National University, annual report 1996 (unpublished), p. 32.
- [29] M. Pautrat, J. M. Lagrange, A. Viridis, J. S. Dionisio, Ch. Vieu, and J. Vanhorenbeeck, *Phys. Scr.* **34**, 378 (1986).
- [30] B. Fant, R. J. Tanner, P. A. Butler, A. N. James, G. D. Jones, R. J. Poynter, C. A. White, K. L. Ying, D. J. G. Love, J. Simpson, and K. A. Connell, *J. Phys. G* **17**, 319 (1991).
- [31] M. Kaci *et al.*, *Z. Phys. A* **354**, 267 (1996).
- [32] J. J. van Ruyven, J. Penninga, W. H. A. Hesselink, P. Van Nes, K. Allaart, E. J. Engeveld, H. Verheul, M. J. A. De Voigt, Z. Sujkowski, and J. Blomqvist, *Nucl. Phys. A* **449**, 579 (1986).
- [33] M. Pautrat, J. M. Lagrange, J. S. Dionisio, Ch. Vieu, and J. Vanhorenbeeck, *Nucl. Phys. A* **443**, 172 (1985).
- [34] U. Rosengård, P. Carlé, A. Källberg, L. O. Norlin, K.-G. Rensfelt, H. C. Jain, B. Fant, and T. Weckström, *Nucl. Phys. A* **482**, 573 (1988).
- [35] M. Pautrat, J. M. Lagrange, J. S. Dionisio, Ch. Vieu, and J. Vanhorenbeeck, *Nucl. Phys. A* **484**, 155 (1988).